

NIR-to-blue, green, orange and white up-conversion luminescence in $\text{Yb}^{3+}/\text{Tm}^{3+}/\text{Er}^{3+}/\text{Ho}^{3+}$ -doped $\text{Na}_{0.5}\text{Gd}_{0.5}\text{WO}_4$ nanocrystals

ZHIGUO XIA^{*}, HAIYAN DU^a, JIAYUE SUN^a

School of Materials Sciences and Technology, China University of Geosciences, Beijing 100083, China

^aCollege of Chemistry and Environmental Engineering, Beijing Technology and Business University, Beijing 100048, China

$\text{Yb}^{3+}/\text{Tm}^{3+}/\text{Er}^{3+}/\text{Ho}^{3+}$ -doped $\text{Na}_{0.5}\text{Gd}_{0.5}\text{WO}_4$ nanocrystals have been fabricated by a facile hydrothermal method. The blue, green and orange upconversion (UC) emissions coming from $\text{Yb}^{3+}/\text{Tm}^{3+}$, $\text{Yb}^{3+}/\text{Er}^{3+}$, $\text{Yb}^{3+}/\text{Ho}^{3+}$ dopant ions are observed in this study. Bright white luminescence upon 980 nm excitation can be produced via the UC process by tuning the dopant ions $\text{Yb}^{3+}/\text{Tm}^{3+}/\text{Ho}^{3+}$, which consists of the blue, green and red UC emissions, and they correspond to the transitions $^1\text{G}_4 \rightarrow ^3\text{H}_6$ of Tm^{3+} , $^5\text{F}_4(^5\text{S}_2) \rightarrow ^5\text{I}_6$, and $^5\text{F}_5 \rightarrow ^5\text{I}_6$ of Ho^{3+} ions, respectively. The UC mechanisms and temperature dependent UC luminescence were also discussed.

(Received March 1, 2010; accepted May 26, 2010)

Keywords: Optical materials; Phosphors, Upconversion luminescence, Optical properties

1. Introduction

Recently, there are extensively investigations on upconversion (UC) luminescence materials due to their application in many advanced technology fields, such as displays, lasers, photonics, and biomedicine [1-3]. Among the UC rare-earth ions, it is well known that Yb^{3+} ion is a good sensitizer which can greatly enhance UC efficiency through energy transfer owing to the strong absorption in the region around 980 nm [4]. Accordingly, Er^{3+} , Tm^{3+} and Ho^{3+} ions are the most important active ions applied to UC luminescence, because of their favorable energy level structure [4-6]. Recently, a growing interest has been focused on white light-emitting diodes (w-LEDs), especially phosphor-converted w-LEDs [7]. Since photon UC can also be used for the generation of visible emission by near infrared (NIR) excitation of Ln^{3+} -doped materials, the strategy on developing materials that can be excited with commercially available NIR diode lasers has been proved to be very promising [8]. Some efforts have been made to develop white light emission Ln^{3+} -doped materials via UC process. Sivakumar [9] reported the white UC luminescence SiO_2 , ZrO_2 sol-gel thin film made with Ln^{3+} (Tm^{3+} , Er^{3+} , Eu^{3+})-doped LaF_3 nanoparticles codoped with Yb^{3+} ions. After that, single-phase rare earth oxides matrices, such as Y_2O_3 [8], Lu_2O_3 [10], $\text{Lu}_3\text{Ga}_5\text{O}_{12}$ [11], YAlO_3 [12], $\text{Gd}_2(\text{MoO}_4)_3$ [13] and $\text{La}_2(\text{MoO}_4)_3$ [14] have also reported as white UC luminescence host, which is relation to the combination of upconverted blue (from Tm^{3+}), green (from Er^{3+}), and red (from $\text{Er}^{3+}/\text{Ho}^{3+}$) emissions resulted in the white luminescence.

The host materials also play an important role in obtaining highly efficient UC luminescence. It is widely

accepted that NIR to visible UC emission in fluoride materials has been observed with better efficiency [1, 15]. However, due to their hygroscopic nature, their applications are limited. However, among the reported oxide materials as the UC host, tungstate and molybdate are two families as the potential hosts with better UC efficiency [13-14]. Moreover, they have high chemical and thermal durability, and are therefore suitable material for technological applications. Based on this, we firstly report the $\text{Yb}^{3+}/\text{Tm}^{3+}/\text{Er}^{3+}/\text{Ho}^{3+}$ -doped $\text{Na}_{0.5}\text{Gd}_{0.5}\text{WO}_4$ nanocrystals prepared by the mild hydrothermal method in this work, and the blue, green, orange and white UC luminescence properties and mechanisms were discussed in detail.

2. Experimental

The $\text{Yb}^{3+}/\text{Tm}^{3+}$, $\text{Yb}^{3+}/\text{Er}^{3+}$, $\text{Yb}^{3+}/\text{Ho}^{3+}$, and $\text{Yb}^{3+}/\text{Tm}^{3+}/\text{Ho}^{3+}$ -doped $\text{Na}_{0.5}\text{Gd}_{0.5}\text{WO}_4$ UC materials were prepared by a facile hydrothermal method. The starting materials were Na_2CO_3 (A.R.), $5(\text{NH}_4)_2\text{O} \cdot 12\text{WO}_3 \cdot 5\text{H}_2\text{O}$ (A.R.), Gd_2O_3 (99.99%), Yb_2O_3 (99.99%), Tm_2O_3 (99.99%) and Ho_2O_3 (99.99%). For a typical synthesis of 10% Yb^{3+} /1% Tm^{3+} /0.4% Ho^{3+} -doped $\text{Na}_{0.5}\text{Gd}_{0.5}\text{WO}_4$ nanocrystals, the calculated starting compositions are as follows, $0.25 \text{Na}_2\text{CO}_3 + 1/12 5(\text{NH}_4)_2\text{O} \cdot 12\text{WO}_3 \cdot 5\text{H}_2\text{O} + 0.193 \text{Gd}_2\text{O}_3 + 0.05 \text{Yb}_2\text{O}_3 + 0.005 \text{Tm}_2\text{O}_3 + 0.002 \text{Ho}_2\text{O}_3$. Firstly, stoichiometric amounts of Gd_2O_3 , Yb_2O_3 , Tm_2O_3 and Ho_2O_3 were dissolved in dilute HNO_3 (A.R.) under vigorous stirring, resulting in the formation of a colorless solution. After evaporation followed by drying at 100 °C

for 12 h in ambient atmosphere, a powder of rare earth nitrate $\text{RE}(\text{NO}_3)_3$ was obtained. Then Solution A was obtained by adding some amounts of deionized water to $\text{RE}(\text{NO}_3)_3$. Solution B was prepared by dissolving the stoichiometric amount of Na_2CO_3 and $5(\text{NH}_4)_2\text{O} \cdot 12\text{WO}_3 \cdot 5\text{H}_2\text{O}$ in a suitable volume of deionized water, and stirred homogeneously. Solution B was then added dropwise to solution A with vigorous magnetic stirring. The formed suspension was stirred continuously for 1 h, and then transferred to a Teflon-lined autoclave of 50 ml capacity, sealed and heated at 160°C for 8 h. It was then cooled to room temperature naturally. The white precipitate was separated centrifugation and washed with deionized water and ethanol several times. The final product was obtained after drying at 80°C for 12 h.

The phase structure of the as-synthesized UC materials were determined by X-ray powder diffraction spectroscopy (XRD, using a Shimadzu XRD-6000) operating at Cu $K\alpha$ radiation, 40 kV, 30 mA, and a scan speed of 2.0° (2 θ)/min. Transmission electron microscope (TEM) images were observed using a JEOL-2010 Electron Microscope with an acceleration voltage of 120 kV. The UC luminescence spectra were recorded on a Hitachi F-4500 spectrophotometer equipped with an external power-controllable 980 nm semiconductor laser (Beijing Viasho Technology Company, China) as the excitation source, which is connected with an optic fiber accessory. The temperature dependence UC spectra were measured by the same equipment as above, which was then combined with a self-made heating attachment and a computer-controlled electric furnace.

3. Results and discussion

3.1 Structure characterization of $\text{Yb}^{3+}/\text{Tm}^{3+}/\text{Er}^{3+}/\text{Ho}^{3+}$ -doped $\text{Na}_{0.5}\text{Gd}_{0.5}\text{WO}_4$ nanocrystals

Fig. 1 gives the XRD pattern of as-prepared $\text{Na}_{0.5}\text{Gd}_{0.5}\text{WO}_4:10\%\text{Yb}^{3+}, 1\%\text{Tm}^{3+}, 0.4\%\text{Ho}^{3+}$ nanocrystals. It is also found from Fig. 1a that the peak positions agree well with those of the standard pattern (JCPDS NO. 25-0829) for $\text{Na}_{0.5}\text{Gd}_{0.5}\text{WO}_4$ in scheelite structure, which has an tetragonal phase with the lattice constants of $a = 5.243 \text{ \AA}$, $c = 11.36 \text{ \AA}$, and v (cell volume) = 312.50 \AA^3 . Further, from the XRD pattern, it also can be concluded that the sample is well crystallized, and the grain size can be calculated using the Debye-Scherrer equation: $D = K\lambda/\beta\cos\theta$. By using the strongest diffraction peak (112) at 28.9° , the obtained grain size for the as-synthesized UC material is about 105 nm.

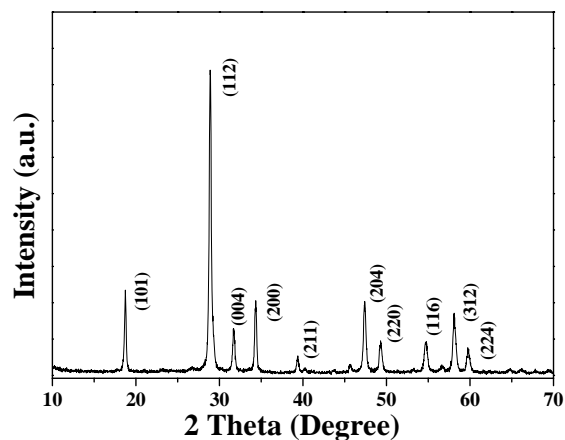


Fig. 1. XRD pattern of as-prepared $\text{Na}_{0.5}\text{Gd}_{0.5}\text{WO}_4:10\%\text{Yb}^{3+}, 1\%\text{Tm}^{3+}, 0.4\%\text{Ho}^{3+}$ nanocrystals.

Fig. 2 shows the TEM image of as-prepared $\text{Na}_{0.5}\text{Gd}_{0.5}\text{WO}_4:10\%\text{Yb}^{3+}, 1\%\text{Tm}^{3+}, 0.4\%\text{Ho}^{3+}$ nanocrystals by using different scale, and it is found that the obtained $\text{Na}_{0.5}\text{Gd}_{0.5}\text{WO}_4$ particles has rectangle like shape, and the average grains diameter is about 100 nm. As also given in Fig. 2 (b), the enlarged TEM image further reflects the rectangle like shape morphology. It verified the characteristic growth of the $\text{Na}_{0.5}\text{Gd}_{0.5}\text{WO}_4$ with tetragonal phase microstructure. The observed grains diameter is also consistent with the calculation result by the Debye-Scherrer.

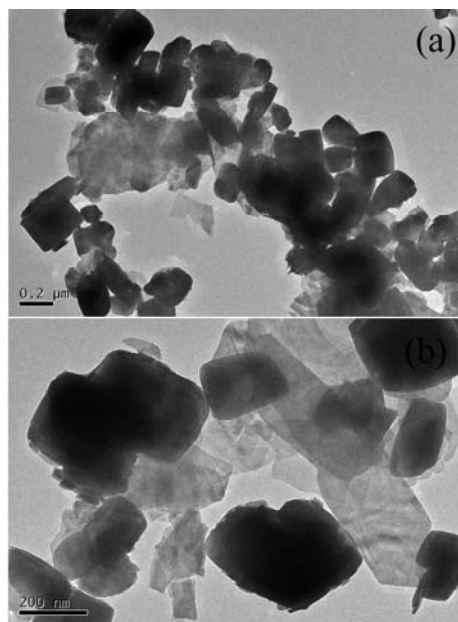


Fig. 2. TEM images of as-prepared $\text{Na}_{0.5}\text{Gd}_{0.5}\text{WO}_4:10\%\text{Yb}^{3+}, 1\%\text{Tm}^{3+}, 0.4\%\text{Ho}^{3+}$ nanocrystals, (a) $0.2 \mu\text{m}$ scale, (b) 200 nm scale.

3.2 UC luminescence properties analysis of Yb³⁺/Tm³⁺/Er³⁺/Ho³⁺-doped Na_{0.5}Gd_{0.5}WO₄ nanocrystals

Fig. 3 gives the UC luminescence spectra of Na_{0.5}Gd_{0.5}WO₄ nanocrystals doped with 10%Yb³⁺/1%Tm³⁺, 10%Yb³⁺/1%Er³⁺, and 10%Yb³⁺/1%Ho³⁺ under 980 nm semiconductor laser excitation. It is found that the blue (473 nm), green (528 nm and 550 nm), and orange (543 nm and 655 nm) UC emission bands, which correspond to the transitions ¹G₄ → ³H₆ of Tm³⁺, ²H_{11/2}, ⁴S_{3/2} → ⁴I_{15/2} of Er³⁺, ⁵F₄(⁵S₂) → ⁵I₈, and ⁵F₅ → ⁵I₈ of Ho³⁺ ions, respectively, can be found. It is noticed that the orange emission of Ho³⁺ comes from the blend mode of the green and red UC emission light. Further, as seen in Fig. 3d, by adjusting relative amounts of the rare earth dopant ions, 10%Yb³⁺/1%Tm³⁺/0.4%Ho³⁺-doped Na_{0.5}Gd_{0.5}WO₄ sample shows bright white UC luminescence, which consists of the blue (473 nm), green (543 nm), and red (655 nm) UC emissions, and they correspond to the transitions ¹G₄ → ³H₆ of Tm³⁺, ⁵F₄(⁵S₂) → ⁵I₈, and ⁵F₅ → ⁵I₈ of Ho³⁺ ions, respectively. Furthermore, we also calculated the CIE chromaticity coordinates of the above four kinds of phosphors based on their corresponding UC luminescence spectra, which were represented in Fig. 4. It was found that the CIE chromaticity coordinates for 10%Yb³⁺/1%Tm³⁺ (a), 10%Yb³⁺/1%Er³⁺ (b), 10%Yb³⁺/1%Ho³⁺ (c), 10%Yb³⁺/1%Tm³⁺/0.4%Ho³⁺ (d) doped Na_{0.5}Gd_{0.5}WO₄ phosphors were (x = 0.12, y = 0.12), (x = 0.24, y = 0.72), (x = 0.33, y = 0.62) and (x = 0.30, y = 0.33), respectively. Obviously, they were located in the corresponding blue, green, orange and white light region.

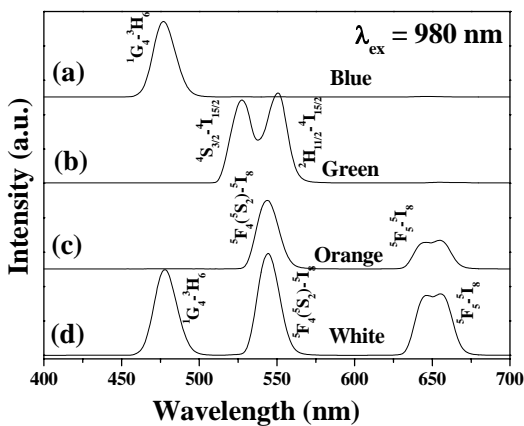


Fig. 3. UC luminescence spectra of Na_{0.5}Gd_{0.5}WO₄ nanocrystals doped with 10%Yb³⁺/1%Tm³⁺ (a), 10%Yb³⁺/1%Er³⁺ (b), 10%Yb³⁺/1%Ho³⁺ (c), and 10%Yb³⁺/1%Tm³⁺/0.4%Ho³⁺ (d) under 980 nm semiconductor laser excitation.

To understand the upconversion mechanisms, the upconversion emission intensity I was measured as a function of the pumped power P [16]. For the upconversion process, I is proportional to the n th power of

P , and that is to say, $I \propto P^n$, where n is the number of pump photons absorbed per upconverted photon emitted. A plot of $\log I$ versus $\log P$ yields a straight line with slope n . Therefore, Fig. 5 gives the pump power dependence of the blue, green, and orange UC luminescence in Na_{0.5}Gd_{0.5}WO₄ nanocrystals doped with Tm³⁺, Er³⁺ and Ho³⁺. As given in Fig. 5, the slope of curve $\lg(I)$ versus $(\lg P)$ was determined to be 2.38, 1.79 (1.75), and 1.86 (1.75) for the blue (Tm³⁺), green (Er³⁺), and orange (Ho³⁺) emissions, respectively, allowing us to propose that two photons process in Er³⁺ and Ho³⁺ UC luminescence processes. And a three photon process was expected for the upconverted blue Tm³⁺ emission.

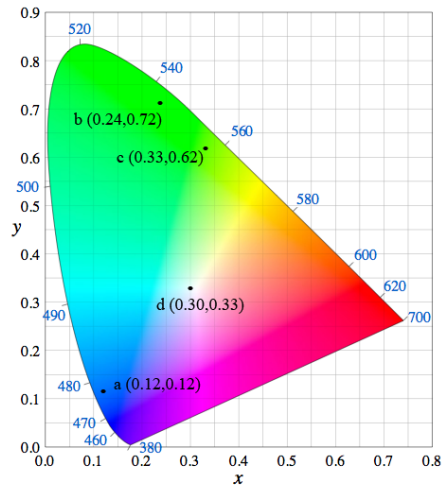


Fig. 4. CIE (X, Y) coordinate diagram (CIE-1931) showing the chromaticity points of the emissions in the Na_{0.5}Gd_{0.5}WO₄ doped with 10%Yb³⁺/1%Tm³⁺ (a), 10%Yb³⁺/1%Er³⁺ (b), 10%Yb³⁺/1%Ho³⁺ (c), and 10%Yb³⁺/1%Tm³⁺/0.4%Ho³⁺ (d) under 980 nm semiconductor laser excitation.

Fig. 6 gives the energy level diagram of the Tm³⁺, Er³⁺, Yb³⁺, and Ho³⁺ ions as well as the proposed upconversion mechanism to produce the blue, green, orange, and white emission for the Yb³⁺/Tm³⁺/Er³⁺/Ho³⁺-doped Na_{0.5}Gd_{0.5}WO₄:10%Yb³⁺,1%Tm³⁺, 0.4%Ho³⁺ nanocrystals upon 980 nm semiconductor laser excitation. As seen in Fig. 6, under the 980 nm excitation, electrons of Yb³⁺ is excited from ²F_{7/2} to ²F_{5/2} level through ground state absorption process, which in turn leads to the energy transfer between Yb³⁺-Tm³⁺, Yb³⁺-Er³⁺ and Yb³⁺-Ho³⁺. Owing to the approximate energy difference between ³H₅ energy level of Tm³⁺ and ⁴I_{11/2} of Er³⁺, the energy transfer can also be expected to form the corresponding transition. The single blue emission bands at 473 can be assigned to ¹G₄ → ³H₆ transitions of Tm³⁺. The two green emission bands at 528 nm and 550 nm are derived from ²H_{11/2} → ⁴I_{15/2} and ⁴S_{3/2} → ⁴I_{15/2} transitions of Er³⁺, respectively. As also found in the UC spectra of 10%Yb³⁺/1%Ho³⁺-doped Na_{0.5}Gd_{0.5}WO₄ nanocrystals, both green and red emission bands can be found, which are corresponding to ⁵F₄(⁵S₂) →

5I_8 , and $^5F_5 \rightarrow ^5I_8$ transitions of Ho^{3+} ions, respectively. This above mechanism is in good agreement with the calculated slopes, which also reflects the possible luminescence process that pump photons absorbed in it.

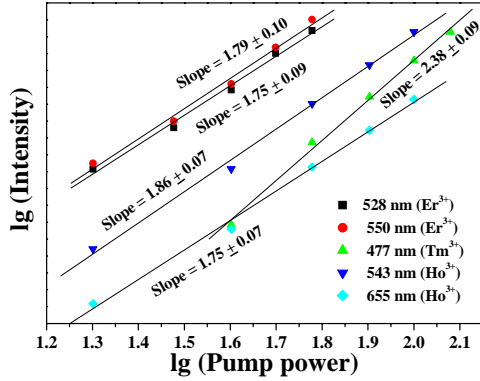


Fig. 5. Pump power dependence of the blue, green, and orange UC luminescence in $\text{Na}_{0.5}\text{Gd}_{0.5}\text{WO}_4$ nanocrystals doped with Tm^{3+} , Er^{3+} and Ho^{3+} .

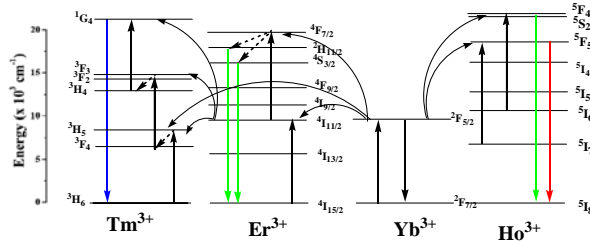


Fig. 6. Energy level diagram of the Tm^{3+} , Er^{3+} , Yb^{3+} , and Ho^{3+} ions as well as the proposed upconversion mechanism to produce the blue, green, orange, and white emission for the $\text{Yb}^{3+}/\text{Tm}^{3+}/\text{Er}^{3+}/\text{Ho}^{3+}$ -doped $\text{Na}_{0.5}\text{Gd}_{0.5}\text{WO}_4$ nanocrystals upon 980 nm semiconductor laser excitation.

3.3 Temperature dependent UC luminescence properties analysis of $\text{Yb}^{3+}/\text{Tm}^{3+}/\text{Er}^{3+}/\text{Ho}^{3+}$ -doped $\text{Na}_{0.5}\text{Gd}_{0.5}\text{WO}_4$ nanocrystals

Fig. 7 shows the UC luminescence spectra of $\text{Na}_{0.5}\text{Gd}_{0.5}\text{WO}_4:10\%\text{Yb}^{3+}, 1\%\text{Tm}^{3+}, 0.4\%\text{Ho}^{3+}$ nanocrystals ($\lambda_{\text{ex}} = 980 \text{ nm}$) at various temperature. It indicates that the emission intensity of the blue, green and red emissions shows similar temperature behavior between the room temperature (20 °C) and 300 °C, and they all decrease with the increasing temperature. Compared to green and red emissions, which correspond to $^5F_4(^5S_2) \rightarrow ^5I_8$, and $^5F_5 \rightarrow ^5I_8$ transitions of Ho^{3+} ions, blue emission originated $^1G_4 \rightarrow ^3H_6$ transitions of Tm^{3+} has the relative weak thermal quenching behavior. As given in Fig. 8, it shows the relative emission intensity of the blue, green, and red UC luminescence as a function of temperature. It is found with increasing temperature up to 200 °C, the normalized

emission intensity of Tm^{3+} is decreased to 73.0% of the initial value, while that of Ho^{3+} is 42.5% for green emission, and 54.6% for red emission.

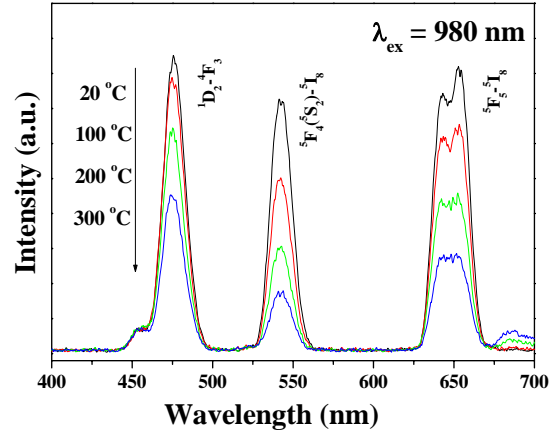


Fig. 7. Temperature dependence of UC luminescence spectra of $\text{Na}_{0.5}\text{Gd}_{0.5}\text{WO}_4:10\%\text{Yb}^{3+}, 1\%\text{Tm}^{3+}, 0.4\%\text{Ho}^{3+}$ nanocrystals upon 980 nm semiconductor laser excitation.

During the increase of temperature, there are two major factors responsible for the decrease of the UC emission. One is an increase of non-radiative relaxation in excited level of activator ions that inhibits radiative emission, which is relative to the thermal equilibrium between neighboring energy levels. The other factor may be the energy migration effect between Yb^{3+} ions which becomes more important at higher temperature [17-18]. However, it is found that the population for two neighboring energy levels is determined by thermal equilibrium, and the rate of non-radiative relaxation increases with the temperature. The transition probability (η) between the different energy levels can be given by the following Eq. (1) [17],

$$\eta \propto [1 - \exp(-\frac{\hbar\omega}{kT})]^{-\Delta E/\hbar\omega} \quad (1)$$

where k is the Boltzmann factor, T is the absolute temperature, $\hbar\omega$ is the phonon energy of the host, and ΔE is the activation energy of non-radiation transition. We can find that $^1G_4 \rightarrow ^3H_6$ transitions of Tm^{3+} corresponding the blue emission has the largest energy difference value, however, it will induces the lowest η value with increasing temperature T , as given by Eq. (1). Further, the effect of temperature on UC emission intensity I can be given by the following Eq. (2) [17, 19],

$$I \propto \frac{I_0 P}{\eta [1 - \exp(-\frac{\hbar\omega}{kT})]^{-\Delta E/\hbar\omega} + P} \quad (2)$$

where P is the sum of all transition probabilities and I_0 is the luminescence intensity at low temperature. From Eq.

(2), we further know that the emission decreases with temperature for a steady-state excitation light, as also given in Fig. 8. Considering that ¹G₄ energy level of Tm³⁺ has the higher energy value corresponding to the excited energy levels, ⁵F₄(⁵S₂) and ⁵F₅ of Ho³⁺ ions, it produced weak thermal quenching behavior with increasing temperature.

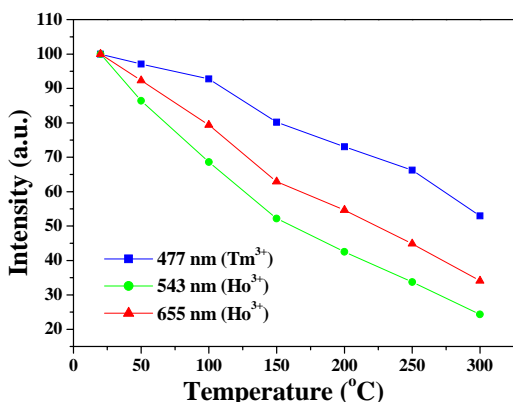


Fig. 8. Relative emission intensities of the blue, green, and red UC luminescence of Na_{0.5}Gd_{0.5}WO₄:10%Yb³⁺,1%Tm³⁺, 0.4%Ho³⁺ nanocrystals as a function of temperature.

4. Conclusions

Yb³⁺/Tm³⁺/Er³⁺/Ho³⁺-doped Na_{0.5}Gd_{0.5}WO₄ nanocrystals were prepared by the facile hydrothermal method, and 10%Yb³⁺/1%Tm³⁺, 10%Yb³⁺/1%Er³⁺, 10%Yb³⁺/1%Ho³⁺, and 10%Yb³⁺/1%Tm³⁺/0.4%Ho³⁺-doped Na_{0.5}Gd_{0.5}WO₄ nanocrystals can produce blue, green, orange and white UC luminescence under 980 nm diode laser excitation, respectively. The blue, green, and orange UC emissions correspond to the transitions ¹G₄ → ³H₆ of Tm³⁺, ²H_{11/2}, ⁴S_{3/2} → ⁴I_{15/2} of Er³⁺, ⁵F₄(⁵S₂) → ⁵I₈, and ⁵F₅ → ⁵I₈ of Ho³⁺ ions, respectively, while bright white luminescence correspond to the combination of the transitions ¹G₄ → ³H₆ of Tm³⁺, ⁵F₄(⁵S₂) → ⁵I₈, and ⁵F₅ → ⁵I₈ of Ho³⁺ ions, respectively. The UC mechanisms and temperature dependent UC luminescence were also proposed in this work. Multicolor UC luminescence nanocrystals promise their potential applications in the field of displays, lasers, photonics, and biomedicine.

Acknowledgements

This study was supported by the Ph.D. Programs Foundation of Ministry of Education of China (Grant No. 20090022120002), the National Natural Science Foundations of China (Grant No. 20876002 and No. 20976002), and the Beijing Natural Science Foundation (Grant No. 2082009 and No. 2091002).

References

- [1] D. Matsuura, Appl. Phys. Lett. **81**, 4526 (2002).
- [2] L. Y. Wang, Y. D. Li, Nano. Lett. **6**, 1645 (2006).
- [3] V. Mahalingam, F. Vetrone, R. Naccache, A. Speghini, J. A. Capobianco, J. Mater. Chem. **19**, 3149 (2009).
- [4] J. L. Yuan, X. Y. Zeng, J. T. Zhao, Z. J. Zhang, H. H. Chen, X. X. Yang, J. Phys. D: Appl. Phys. **41**, 105406 (2008).
- [5] H. Guo, Y. M. Qiao, Opt. Mater. **31**, 583 (2009).
- [6] J. C. Boyer, F. Vetrone, J.A. Capobianco, A. Speghini, M. Bettinelli, Chem. Phys. Lett. **390**, 403 (2004).
- [7] S. Nakamura, M. Senoh, and T. Mukai, Appl. Phys. Lett. **62**, 2390 (1993).
- [8] G. Y. Chen, Y. Liu, Y. G. Zhang, G. Somesfalean, Z. G. Zhang, Q. Sun, F. P. Wang, Appl. Phys. Lett. **91**, 133103 (2007).
- [9] S. Sivakumar, F. C. J. M. Van Veggel, M. Raudsepp, J. Am. Chem. Soc. **127**, 12464 (2005).
- [10] J. Yang, C. Zhang, C. Peng, C. Li, L. Wang, R. Chai, J. Lin, Chem.-Eur. J. **15**, 4649 (2009).
- [11] V. Mahalingam, F. Mangiarini, F. Vetrone, V. Venkatramu, M. Bettinelli, A. Speghini, J. A. Capobianco, J. Phys. Chem. C **112**, 17745 (2008).
- [12] W. C. Lu, X. H. Ma, H. Zhou, G. T. Chen, J. F. Li, Z. J. Zhu, Z. Y. You, and C. Y. Tu, J. Phys. Chem. C **112**, 15071 (2008).
- [13] Y. Pan, Q. Zhang, Mat. Sci. Eng. B-Solid **138**, 90 (2007).
- [14] G. Yi, B. Sun, F. Yang, D. Chen, Y. Zhou, J. Cheng, Chem. Mater. **14**, 2910 (2002).
- [15] Z. Q. Li, Y. Zhang, S. Jiang, Adv. Mater. **20**, 4765 (2008).
- [16] G. Chen, Y. Liu, Y. Zhang, G. Somesfalean, Z. Zhang, Q. Sun, F. Wang, Appl. Phys. Lett. **91**, 133103 (2007).
- [17] M.J. Weber, Phys. Rev. B **8**, 54 (1971).
- [18] Y. Mita, K. Hirama, N. Ando, H. Yamamoto, S. Shionoya, J. Appl. Phys. **74**, 4703 (1993).
- [19] Y. B. Hou, Y. B. Li, X. B. Chen, G. Y. Zhang, Y. Wang, J. Non-Cryst. Solids **260**, 54 (1999).

*Corresponding author: xiazg426@yahoo.com.cn